

ORIGINAL ARTICLE

# The HSV-2 mutant $\Delta$ PK induces melanoma oncolysis through nonredundant death programs and associated with autophagy and pyroptosis proteins

AG Colunga, JM Laing and L Aurelian

Department of Pharmacology and Experimental Therapeutics, University of Maryland, School of Medicine, Baltimore, MD, USA

Malignant melanoma is a highly aggressive and drug-resistant cancer. Virotherapy is a novel therapeutic strategy based on cancer cell lysis through selective virus replication. However, its clinical efficacy is modest, apparently related to poor virus replication within the tumors. We report that the growth compromised herpes simplex virus type 2 (HSV-2) mutant,  $\Delta$ PK, has strong oncolytic activity for melanoma largely caused by a mechanism other than replication-induced cell lysis. The ratio of dead cells (determined by trypan blue or ethidium homodimer staining) to cells that stain with antibody to the major capsid protein VP5 (indicative of productive infection) was 1.8–4.1 for different melanoma cultures at 24–72 h post-infection. Cell death was due to activation of calpain as well as caspases-7 and -3 and it was abolished by the combination of calpain

(PD150606) and pancaspase (benzyloxycarbonyl-Val-Ala-Asp-fluormethyl ketone, z-VAD-fmk) inhibitors. Upregulation of the autophagy protein Beclin-1 and the pro-apoptotic protein H11/HspB8 accompanied  $\Delta$ PK-induced melanoma oncolysis. Intratumoral  $\Delta$ PK injection ( $10^6$ – $10^7$  plaque-forming unit (pfu)) significantly reduced melanoma tumor burden associated with calpain and caspases-7 and -3 activation, Beclin-1 and H11/HspB8 upregulation and activation of caspase-1-related inflammation. Complete remission was seen for 87.5% of the LM melanoma xenografts at 5 months after treatment termination. The data indicate that  $\Delta$ PK is a promising virotherapy for melanoma that functions through virus-induced programmed cell death pathways. Gene Therapy (2010) 17, 315–327; doi:10.1038/gt.2009.126; published online 1 October 2009

**Keywords:** ICP10PK; oncolytic viruses; calpain; caspases; autophagy; pyroptosis

## Introduction

Malignant melanoma is a commonly diagnosed highly aggressive and drug-resistant cancer that accounts for ~75% of cancer skin deaths.<sup>1</sup> Poor prognosis is likely related to the failure of conventional therapies to eradicate cancer stem cells that are responsible for resistance, invasiveness and neoplastic progression.<sup>2</sup> Oncolytic viruses are recognized as a promising novel therapy designed to reduce tumor burden by direct cell lysis resulting from virus replication and the generation of infectious progeny that spreads throughout the tumor.<sup>3,4</sup> Virotherapy may also disrupt the tumor vasculature and induce antitumor immunity,<sup>3,4</sup> and it carries the promise of targeting cancer stem cells.<sup>5</sup> Originally developed to target neuronal cancers, the herpes simplex virus (HSV) oncolytic constructs were generated from HSV-1 through deletion/modification of the neurovirulence protein, ICP34.5, and/or the large subunit of ribonucleotide reductase (R1). Early clinical trials have shown that oncolytic viral therapies are tolerated well, but their efficacy is modest, apparently

related to poor virus replication within the tumors.<sup>6</sup> Accordingly, ongoing efforts have focused on improving virus replication through: (i) fusogenic alterations that increase virus uptake/spread,<sup>7</sup> (ii) modulation of the tumor milieu,<sup>8</sup> (iii) suppression of innate immunity or interference with virus-mediated immune evasion,<sup>9</sup> (iv) expression of immunostimulatory cytokines,<sup>10</sup> and (v) use of cytotoxic drugs in combinatorial therapy.<sup>9,11</sup> However, it is becoming increasingly evident that the development of oncolytic viruses with distinct molecular death functions is highly desirable. Our studies were designed to address this need. They are based on the hypothesis that virotherapy strategies that function through the induction of multiple nonredundant programmed cell death (PCD) pathways provide cancer cell killing selectivity and increase virus spread through the tumor mass<sup>12</sup> while avoiding the replication-related limitations of conventional oncolytic viruses. Development of a PCD-based virotherapy is particularly desirable for melanoma, which is resistant to a wide spectrum of therapeutic modalities,<sup>13</sup> including canonical oncolytic viruses that function through replication-dependent cell lysis<sup>14</sup> and evades immune recognition through its suppressive milieu/potential.<sup>15</sup>

Apoptosis is the best-studied PCD pathway. It is generally mediated by caspases, which are cysteine proteases that are activated by cleavage of precursors or by autocatalysis.<sup>16</sup> Caspase-independent PCD mediated by another protease family known as calpains was

Correspondence: Dr L Aurelian, Department of Pharmacology and Experimental Therapeutics, University of Maryland, School of Medicine, 655 West Baltimore Street, 4-002, Baltimore, MD 21201-1559, USA.

E-mail: laurelia@umaryland.edu

Received 19 February 2009; revised 17 May 2009; accepted 11 June 2009; published online 1 October 2009

also reported.<sup>17</sup> Other PCD pathways include autophagy, which has a major role in cell homeostasis and can cross talk with apoptosis<sup>18</sup> and pyroptosis, a caspase-1-dependent inflammatory process that can activate apoptosis through the pro-inflammatory cytokine tumor-necrosis factor alpha (TNF- $\alpha$ ).<sup>19</sup> Beclin-1, which is required for autophagy induction, acts as a haploinsufficient tumor suppressor protein, the expression of which is inhibited in some human tumors.<sup>20,21</sup>

The HSV type 2 (HSV-2) protein, ICP10 (encoded by the *UL39* gene), has a protein kinase (PK) function that overrides multiple nonredundant PCD pathways in cultured cells and animal models, suggesting that these pathways are likely to be activated by its deletion.<sup>22–27</sup> We focused on the ICP10PK-deleted virus  $\Delta$ PK, because it is known to trigger cell-specific apoptosis<sup>22</sup> and it has strong immunotherapeutic activity mediated by the induction of CD4+ T-helper type 1 (Th1) cells<sup>28</sup> that override the Th2 type response characteristic of melanoma.<sup>29</sup>  $\Delta$ PK also has the distinct advantage that it is tolerated well in human patients.<sup>30,31</sup> Here, we report that  $\Delta$ PK has robust melanoma oncolytic activity in culture and in animal models (xenografts) through the simultaneous activation of multiple nonredundant PCD pathways. These pathways include the activation of distinct proteases and are associated with upregulation of the autophagy protein Beclin-1 and the proapoptotic protein H11/HspB8 previously shown to cause melanoma cell apoptosis<sup>32</sup> and activation of caspase-1-related pyroptosis. To the extent of our knowledge, this is the first report that an HSV oncolytic virus causes tumor cell death by these mechanisms, notably in melanoma.

## Results

### *$\Delta$ PK has tumor-selective growth*

$\Delta$ PK is growth restricted in Vero (African green monkey kidney) cells cultured in low serum, a property associated with its failure to activate Ras signaling pathways.<sup>33,34</sup> As the Ras and B-Raf pathways are activated in most melanoma cultures,<sup>35</sup> we wanted to know whether they compensate for virus growth, providing conditions that enable the tumor selectivity characteristic of oncolytic viruses. We studied a panel of nine human melanoma cultures that includes established (A2058, A375, SKMEL-2, MeWo) and freshly prepared lines (LM, SM, LN, OV, BUL) with different patterns of activated ERK and/or Akt (Supplementary data, Figure S1). Controls were Vero cells, which grow in agarose and cause tumors in animals, at least at a relatively high passage<sup>36</sup> and normal human lung fibroblasts (WI-38) and melanocytes, both of which are primary growth-limited cultures. The cells were infected with  $\Delta$ PK (multiplicity of infection (moi) = 0.5) and assayed for virus growth by plaque assay, as described in Materials and methods. Consistent with previous findings,<sup>33,34</sup> the growth of HSV-2 and the revertant virus HSV-2(R) began at 4 h post-infection (p.i.) and reached a maximal burst size ( $976 \pm 12$  plaque-forming unit (pfu) per cell) at 24 h p.i. By contrast, the growth of  $\Delta$ PK began at 12 h p.i. and reached maximal, albeit low levels ( $1.1 \pm 0.1$  pfu per cell) at 36 h p.i. (Figure 1a). This temporal restriction was released in melanoma cultures, as shown for A2058, MeWo, SM and A375 cells, with growth beginning at 4 h p.i. as determined both by the burst size (pfu per cell)

(Figure 1b) and staining with antibody to the major capsid protein VP5 (Figure 1c). However, the maximal yields of infectious virus ( $1.1 \pm 0.2$  pfu per cell) seen at 18–24 h p.i. were similar to those seen in Vero cells (Figure 1b). The number of VP5+ cells was also relatively low ( $16 \pm 1\%$  at 48 h p.i.) and similar results were obtained for melanoma cultures LM, SKMEL-2, LN, OV and BUL. This was unrelated to the ability of  $\Delta$ PK to infect the cells, because the percentage of cells staining with ICP10 antibody (recognizes the PK deleted ICP10 protein, also known as p95), which is regulated with immediate early (IE) kinetics and is expressed in the absence of VP5,<sup>37,38</sup> was consistent with the rate of infection for the studied moi ( $25 \pm 5\%$  as early as 4 h p.i.) (Figure 1c).  $\Delta$ PK did not grow in WI-38 cells (Figure 1b) but there was a similar percentage of cells staining with ICP10 antibody ( $27 \pm 3\%$ , Figure 1c), indicative of infection. Normal melanocytes behaved like WI-38 cells (data not shown). These findings are in contrast to those obtained for HSV-2 and HSV-2(R), the growth of which was similar to that seen in Vero cells for all the studied cultures ( $921 \pm 54$  and  $737 \pm 28$  pfu per cell, respectively, at 24 h). Collectively, the data indicate that  $\Delta$ PK has selective, albeit relatively low growth potential for transformed/tumor cells.

### *$\Delta$ PK-induced melanoma oncolysis includes a robust component other than virus replication*

The  $\Delta$ PK-infected melanoma cultures were examined for cell death by morphology (cytopathogenic effect (CPE)), trypan blue exclusion and ethidium homodimer-1 (EtHD-1) staining at 0–72 h p.i. Cultures mock-infected with phosphate-buffered saline (PBS) and  $\Delta$ PK-infected freshly isolated normal melanocytes and WI-38 cells were studied in parallel and served as controls.  $\Delta$ PK caused a time-dependent increase in CPE in all the melanoma cultures, with virtually all cells becoming rounded, refractile and detached by 72 h p.i. This was accompanied by increased staining with trypan blue (85–95% positive cells at 72 h p.i.) or EtHD-1 (63–85% positive cells at 72 h p.i.) and similar results were obtained for cultures grown in serum-free medium or in medium supplemented with 10% fetal bovine serum (FBS) (Figures 2a and b). Duplicate cultures obtained at the same times were stained with antibody to VP5 (Figure 1c) and the percentage of dead cells (trypan blue and/or EtHD-1+) was evaluated relative to the percentage of VP5 staining cells. The ratio of trypan blue+ or EtHD-1+/VP5+ cells (Figures 1c and 2) ranged between 1.8 and 4.1 for the different cultures at 24–72 h p.i., with an average of 2.8, suggesting that a major component of cell death is through a program other than lysis caused by productive virus replication (replication bystander effect). In this context, it is important to point out that VP5 also did not colocalize with the terminal deoxynucleotidyl transferase-mediated dUTP nick end labeling (TUNEL), a marker of canonical apoptosis, which was a relatively minor component ( $12.4 \pm 1.1\%$  cells at 48 h p.i.) of the  $\Delta$ PK bystander effect (Supplementary data, Figure S2).  $\Delta$ PK-infected primary melanocytes and WI-38 cells did not stain with trypan blue or EtHD-1 (3.4–5.7% positive cells throughout the study interval) (Figure 2b), supporting the conclusion that  $\Delta$ PK-induced cell death is selective for cancer/transformed cells. Similar results were obtained with virus purified as previously described.<sup>39</sup>

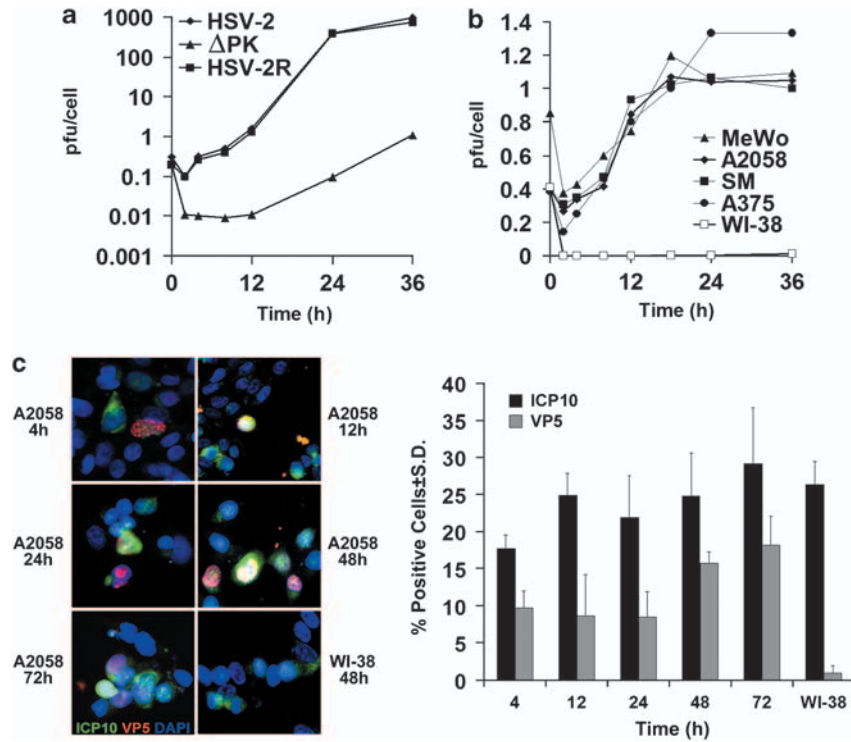


**Figure 1** ΔPK is a growth-restricted replication-competent oncolytic virus. (a) Vero cells were infected with herpes simplex virus type 2 (HSV-2), ΔPK or HSV-2(R) (multiplicity of infection (moi) = 0.5) in serum-free medium, and virus titers were determined by plaque assay. Results are expressed as mean plaque-forming unit per cell (burst size). (b) A2058, MeWo, SM, A375 and WI-38 cells were infected with ΔPK and examined for virus growth as in panel a. Similar growth patterns were seen in melanoma cultures LM, SK-MEL-2, LN, OV and BUL. ΔPK did not grow in WI-38 cells and in normal melanocytes, but HSV-2 and HSV-2(R) replicated equally well in all the cultures. (c) ΔPK-infected A2058 and WI-38 cells were stained with Alexafluor-488-labeled ICP10 and Alexafluor-594-labeled VP5 antibodies in double immunofluorescence. As described in Materials and methods, ICP10 antibody recognizes both the wild-type protein and the PK-deleted ICP10 protein, p95. Cells were counted in three randomly selected fields ( $\geq 250$  cells) and the percentage of staining cells was calculated relative to total cells identified by 4,6-diamidino-2-phenylindole (DAPI) staining. Quantitative results are shown for A2058 cell at 4–72 h post-infection (p.i.), and for WI-38 cells at 48 h p.i. Similar results were obtained for the partially purified virus.

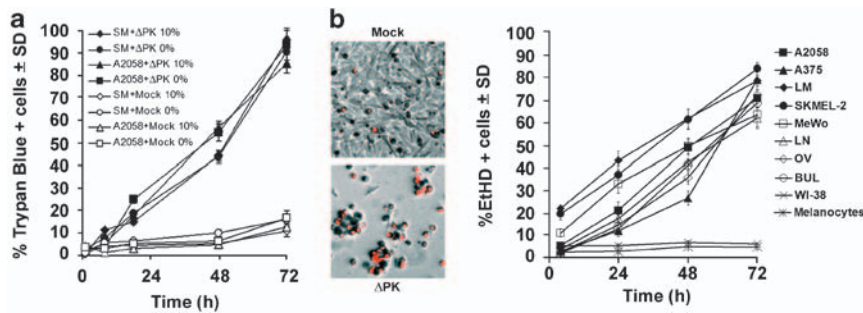


**Figure 2** ΔPK-mediated melanoma oncolysis includes a robust programmed cell death (PCD) bystander component. (a) A2058 and SM melanoma cultures infected with ΔPK (multiplicity of infection (moi) = 0.5, closed symbols) or mock-infected with adsorption medium (open symbols) were cultured in medium without (0%) or with (10%) fetal bovine serum and cells were stained with trypan blue at various times post-infection (p.i.) Four independent hemocytometer counts were performed and percentage of staining cells was calculated. Results from three replicate experiments are expressed as mean percentage of staining cells. (b) Melanoma, primary normal melanocytes and normal fibroblasts (WI-38) infected and cultured in serum-free medium were stained with ethidium homodimer-1 (EtHD-1). Cells were counted in three randomly selected fields ( $\geq 250$  cells) and the percentage of staining cells was calculated as in panel a. The image panels are mock- or ΔPK-infected A2058 cells at 72 h p.i. and are representative of all the melanoma cultures. Similar results were obtained for the partially purified virus.

### Calpain and caspases-7 and -3 are activated in ΔPK-infected melanoma cultures

Having seen that ΔPK-mediated melanoma cell death includes a component other than virus replication, we considered the possibility that this component involves PCD. We considered caspases-3 and -7, which occupy

nonredundant roles within the cell death machinery<sup>40</sup> and calpains, which act through different PCD pathways independently or in cooperation with the caspases.<sup>17,27</sup> Extracts of melanoma cells infected with ΔPK for 0–24 h were immunoblotted with antibodies to calpain and caspases-7 and -3, and the results were quantitated by densitometric scanning, as described in Materials and

methods. As shown for A2058 cells,  $\Delta$ PK caused sequential and apparently independent activation of these three proteases. Calpain activation, expressed as an increased ratio of the active (p76) to inactive (p80) forms of the catalytic subunit, was first seen at 1 h p.i. and it was followed at 24 h p.i. by the loss of the p28 regulatory subunit, which is another marker of enzyme activation<sup>41</sup> (Figure 3a). Activation of caspase-7 was first seen at 4 h p.i., as evidenced by the appearance of the caspase-7p20 cleavage product, and it continued with time p.i., with the smaller p17 and p11 breakdown products seen at 24 h p.i. Activation of caspase-3 was first seen at 24 h p.i., and it appeared to be less robust than that seen for caspase-7,

as determined by the levels of the respective cleavage products (Figure 3b).

As calpain can attenuate or facilitate the activity of the caspases<sup>42,43</sup> and it is activated before them, we wanted to know whether calpain activation contributes to the ability of  $\Delta$ PK to activate the caspases. Extracts from duplicate cultures infected with  $\Delta$ PK in the absence or presence of the calpain inhibitor, PD150606 (100  $\mu$ M), were immunoblotted with antibodies to calpain followed by caspases-7 and -3. Calpain activation was inhibited by PD150606, as evidenced by reduced p76/p80 ratios and retention of p28 (Figure 3a). By contrast, the levels of the caspase cleavage products (caspase-7p17 and p11

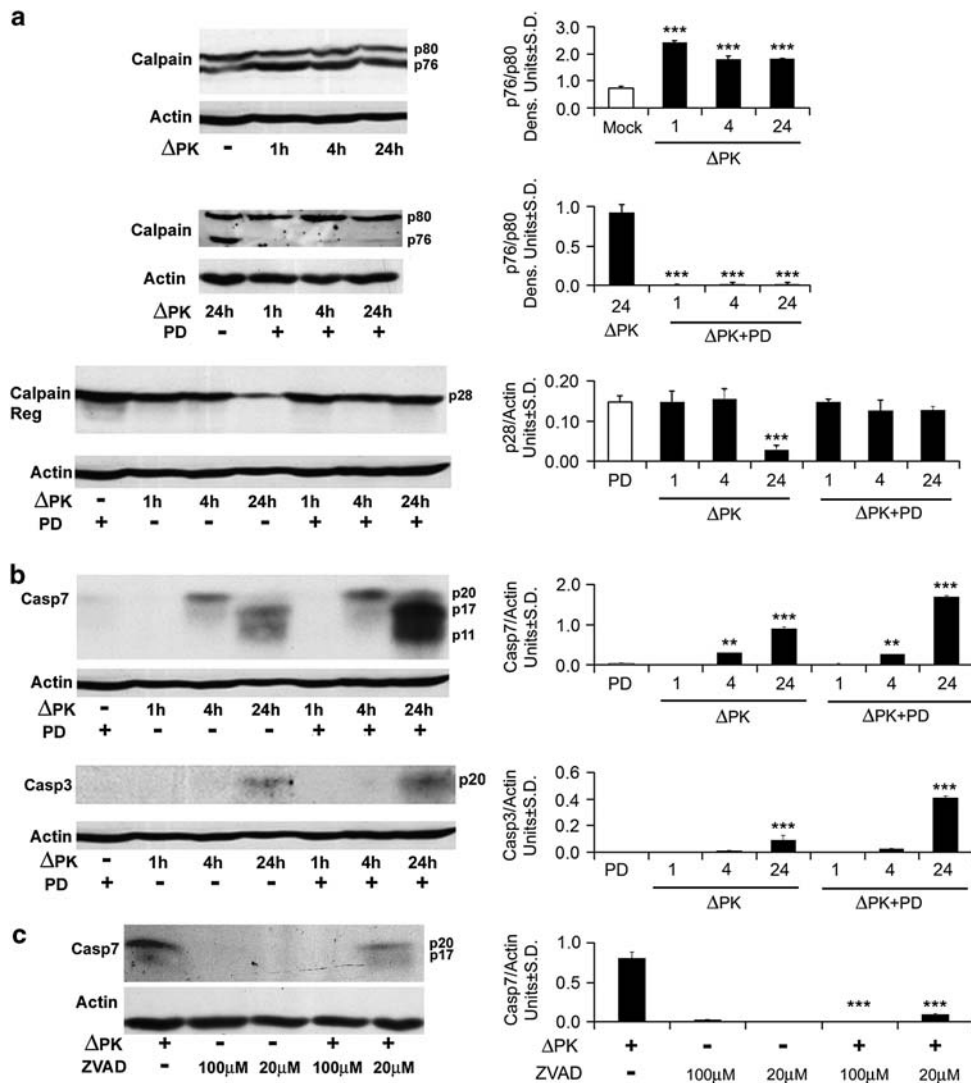


**Figure 3** Calpain and caspases-7 and -3 are activated in  $\Delta$ PK-infected melanoma cells. (a) A2058 cells were infected with  $\Delta$ PK (multiplicity of infection (moi)=0.5) or mock-infected with phosphate-buffered saline in the absence or presence of the calpain inhibitor PD150606 (100  $\mu$ M) and cell extracts obtained at various times post-infection (p.i.) were immunoblotted with antibody to calpain that recognizes the inactive (p80) and activated (p76) species. Data were quantified by densitometric scanning, as described in Materials and methods and results are expressed as the ratio of the p76/p80 densitometric units  $\pm$  s.d. The extracts were also immunoblotted with antibody to the calpain p28 regulatory subunit. Data were quantified by densitometric scanning and results are expressed as densitometric units  $\pm$  s.d. Representatives of three replicate experiments are shown (\*\* $P < 0.001$  vs mock). (b) The immunoblots examined for p28 expression in panel a were sequentially stripped and re-probed with antibodies to activated caspase-7, activated caspase-3 and actin. Data were quantified by densitometric scanning, as described in Materials and methods, and results are expressed as densitometric units  $\pm$  s.d. (\*\* $P < 0.01$ , \*\*\* $P < 0.001$  vs mock). (c) Extracts of A2058 melanoma cells infected with  $\Delta$ PK (moi=0.5) with or without benzylloxycarbonyl-Val-Ala-Asp-fluormethyl ketone (z-VAD-fmk) (Sigma-Aldrich, 100  $\mu$ M or Promega, 20  $\mu$ M) were obtained at 24 h p.i. and immunoblotted with antibody to activated caspase-7. Representatives of three replicate experiments are shown (\*\* $P < 0.001$  vs  $\Delta$ PK alone).

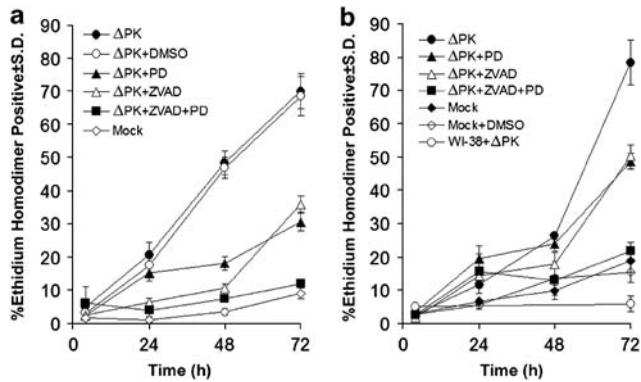


**Figure 4**  $\Delta$ PK-induced melanoma cell death is both calpain and caspase dependent. (a) A2058 cells were infected with  $\Delta$ PK (multiplicity of infection (moi)=0.5) or mock-infected with phosphate-buffered saline and cultured without or with PD150606 (100  $\mu$ M), benzoyloxycarbonyl-Val-Ala-Asp-fluormethyl ketone (z-VAD-fmk) (20  $\mu$ M) or both PD150606 and z-VAD-fmk. DMSO (28 mM) was used as vehicle control. Replicate cultures ( $n=3$ ) were stained with ethidium homodimer-1 (EtHD-1) at various times post-infection and the percentage of staining cells was calculated as in Figure 2. (b) A375 cells were infected with  $\Delta$ PK (moi=0.5) in the absence or presence of inhibitors and stained with EtHD-1+ as in panel a.  $\Delta$ PK-infected WI-38 cells and mock-infected DMSO-treated cells served as controls.

and caspase-3p17) were increased, at least at 24 h p.i. (Figure 3b). This is not a technical artifact, because caspase activation was inhibited by the pancaspase inhibitor, benzoyloxycarbonyl-Val-Ala-Asp-fluormethyl ketone (z-VAD-fmk) (100  $\mu$ M, Sigma-Aldrich (St Louis, MO, USA); 20  $\mu$ M Promega (Madison, WI, USA)), as shown for caspase-7 in Figure 3c. z-VAD-fmk did not affect calpain activation, and neither PD150606 nor z-VAD-fmk had any effect on virus growth (data not shown). Similar results were obtained for all the studied melanoma cultures, both in terms of protease activation and its inhibition. Collectively, the data indicate that calpain reduces, but does not abrogate the ability of  $\Delta$ PK to cause caspase activation, supporting the interpretation that these are independent events.

#### *$\Delta$ PK-induced oncolysis is calpain and caspase dependent*

To examine the role of the activated proteases in  $\Delta$ PK-induced melanoma cell death, the cultures were mock-infected with PBS or infected with  $\Delta$ PK in the absence or presence of PD150606 or/and z-VAD-fmk and cell death was determined at 0–72 h p.i. by EtHD-1 staining. As shown in Figure 4 for A2058 and A375 cells,  $\Delta$ PK caused a time-dependent increase in the percentage of EtHD-1+ cells that reached maximal levels at 72 h p.i. ( $70.1 \pm 5.4$  and  $78.4 \pm 6.8\%$ , respectively). This percentage was significantly decreased by PD150606 ( $30.7 \pm 2.8$  and  $49.1 \pm 2.5\%$  for A2058 and A375 cells, respectively) or z-VAD-fmk ( $35.8 \pm 2.5$  and  $49.6 \pm 3.7\%$  for A2058 and A375 cells, respectively), but cell death was abrogated in cells treated with the combination of both inhibitors. The data indicate that calpain and caspase activation contribute to  $\Delta$ PK-induced melanoma oncolysis in an additive manner, supporting the conclusion that the two death pathways function independently.

#### *$\Delta$ PK inhibits the growth of melanoma xenografts*

To examine whether  $\Delta$ PK has oncolytic activity in melanoma xenografts, A2058, A375 and LM cells were implanted into Balb/c nude mice by subcutaneous injection into both flanks. The animals were given intratumoral injections (100  $\mu$ l) of partially purified  $\Delta$ PK ( $10^6$  and  $10^7$  per injection) or culture medium control. A total of four injections were given at weekly intervals beginning when the tumors were palpable ( $\sim 200$  mm<sup>3</sup>, day 14 for A2058 and day 7 for A375 and LM xenografts). The virus dose is unrelated to the specific cell line in which it was used and was chosen in order to determine an efficacy range. Tumor volume was calculated as described in Materials and methods. All the mock-treated xenografts evidenced time-dependent growth, with A2058 reaching maximal volume at 42 days (Figure 5a), A375 at 35 days (Figure 5b) and LM at 28 days (Figure 5c), when the mice were killed.  $\Delta$ PK caused a significant ( $P < 0.001$ ) decrease in the growth of all the tumors. In the case of the LM xenografts, complete remission was seen for seven of eight tumors (87.5%) followed for 5 months after the last  $\Delta$ PK injection (Figure 5c). The lone recurrent tumor (seen in one animal) did not reach end-point criteria (1.5 cm in diameter) by this time. Compared with the mock-treated animals, survival was significant ( $P < 0.001$ ), ranging between 80% for A2058 and 100% for LM xenografts, as shown for the latter in Figure 5d.

#### *Inhibition of tumor growth is associated with low levels of sustained virus replication and calpain/caspase activation*

Mock- and  $\Delta$ PK-treated xenograft tissues were collected at 7 days after the last  $\Delta$ PK injection and tissue homogenates were examined for virus replication (infectious virus titers) and activation of calpain and caspases-7 and -3, as described in Materials and methods. Virus titers in the  $\Delta$ PK-treated tissues ranged between  $2 \times 10^2$  and  $1.5 \times 10^5$  pfu ml<sup>-1</sup>. In addition, serial sections encompassing the entire tumor mass stained with VP5 antibody with  $\sim 18$ –25% VP5+ cells per section, indicative of relatively good virus penetration. Virus was not isolated from the mock-treated tissues and they did not stain with VP5 antibody (Supplementary data, Figure S3). Calpain and caspases-7 and -3 were activated in  $\Delta$ PK- but not mock-treated tissues, as evidenced by: (i) increased ratios of the calpain p76/p80 isoforms, (ii) loss of the p28 regulatory subunit, (iii) presence of the caspase-7p20 and p17 cleavage fragments, and (iv) loss of pro-caspase-3p30 (Figure 6). Protease activation is due to  $\Delta$ PK and is not an artifact caused by differences in the tumor microenvironment, because activation was not observed in mock-treated tumors and the proteases were also activated by  $\Delta$ PK in cultured melanoma cells. Collectively, the data indicate that  $\Delta$ PK replicates at relatively low but sustained levels (still seen at 7 days p.i.) in the melanoma xenografts, in which it triggers activation of calpain, as well as caspases-7 and -3.

#### *$\Delta$ PK upregulates Beclin-1 and H11/HspB8 in melanoma cultures and xenografts*

Two series of experiments were carried out in order to examine whether  $\Delta$ PK-induced cell death is also

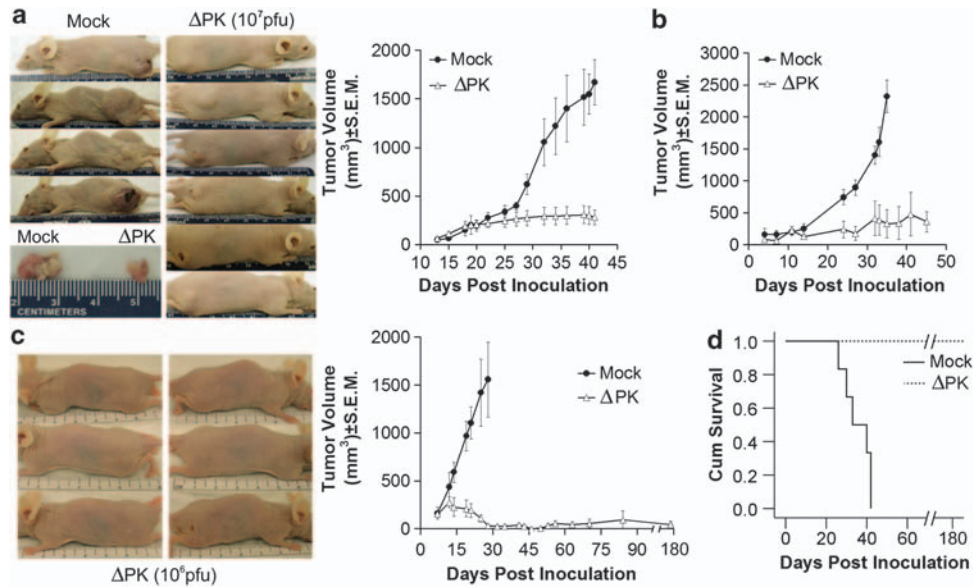


**Figure 5** ΔPK inhibits the growth of melanoma xenografts. (a) A2058 melanoma cells ( $10^7$ ) were implanted subcutaneously into both flanks of Balb/c nude mice and given intratumoral (i.t.) injections (100  $\mu$ l) of ΔPK ( $n=12$ ;  $10^7$  plaque-forming unit (pfu)) or growth medium ( $n=6$ ; mock) beginning on day 14, when the tumors were palpable ( $\sim 200$  mm<sup>2</sup>). A total of four injections were given once weekly and tumor volume was calculated as described in Materials and methods. The difference between mock- and ΔPK-treated animals became statistically significant on day 32 ( $P<0.001$  by two-way analysis of variance (ANOVA)) and remained significant to the end of the study. Representative animals and tumor tissues were photographed at day 42. (b) A375 xenografts were established as in panel a and were given four i.t. injections of ΔPK ( $n=6$ ;  $10^6$  pfu) or growth medium ( $n=6$ ) at weekly intervals beginning on day 7, when the tumors were palpable. The difference between mock and ΔPK treatment became statistically significant at day 23 and remained significant by the end of the study ( $P<0.001$  by two-way ANOVA). (c) LM melanoma cells ( $10^7$ ) were implanted subcutaneously into both flanks of Balb/c nude mice and were given four i.t. injections of ΔPK ( $n=6$ ;  $10^6$  pfu) or growth medium ( $n=6$ ; mock) at weekly intervals beginning on day 7, when the tumors were palpable. Tumor volume in four animals was monitored for 5 months after the last ΔPK injection. The difference between mock and ΔPK treatment became statistically significant on day 14 ( $P<0.001$  by two-way ANOVA) and remained significant to the end of the study. Three ΔPK-treated mice showing complete tumor eradication were photographed at day 35. (d) Kaplan-Meier survival analysis in animals given LM xenografts with the terminal event set at 1.5 cm diameter of growth in any one direction. ΔPK is significantly different from mock ( $P<0.001$ ) by Log-Rank (Mantel-Cox) analysis.

associated with the activation of other death pathways. In the first series, extracts of A2058 cell cultures mock-infected or infected with ΔPK were immunoblotted with antibodies to the autophagy protein Beclin-1 and the heat shock protein H11/HspB8. Beclin-1 is a critical autophagy protein that is emerging as a potent tumor suppressor and is downregulated in some human tumors.<sup>20,21</sup> Its expression in melanoma is unknown. H11/HspB8 is a small heat shock protein that is silenced in 50–60% of melanomas and triggers apoptosis on forced expression.<sup>32</sup> The data summarized in Figures 7a and b indicate that Beclin-1 was minimally expressed in mock-infected cultures and there was no expression of H11/HspB8. ΔPK upregulated both Beclin-1 and H11/HspB8, with the expression first seen at 1 and 4 h p.i., respectively. The second series of experiments examined Beclin-1 and H11/HspB8 expression in melanoma xenografts. Beclin-1 expression was inhibited in four of six mock-treated tumors and ΔPK caused its upregulation in all the studied xenografts (Figure 7c). H11/HspB8 expression was also inhibited in the mock-treated xenografts and upregulated in three of five of those treated with ΔPK (Figure 7d). Beclin-1 and H11/HspB8 upregulation is not an artifact caused by the tumor microenvironment, because it was also seen in cultured melanoma cells and it was not seen in the mock-infected tumors.

#### Caspase-1-related inflammation is associated with ΔPK oncolysis

Pyroptosis is a caspase-1-dependent inflammatory form of cell death that involves formation of the inflammasome complex and was originally observed in macrophages.<sup>44,45</sup> As ΔPK induces production of the pro-inflammatory cytokine TNF- $\alpha$  in the macrophage-related microglial cells,<sup>46</sup> we wanted to know whether ΔPK-induced oncolysis is also associated with inflammatory processes, which are a known component of apoptosis. Duplicates of the mock- and ΔPK-treated xenografts were stained with antibodies to activated caspase-1, CD11b (macrophage marker) and TNF- $\alpha$ , which is known to activate caspase-1,<sup>19</sup> trigger apoptosis and slow the growth of some tumors.<sup>47</sup> Staining with all three antibodies was seen in the ΔPK, but not mock-treated tissues (Figure 8), indicating that caspase-1 activation and inflammation, both of which are considered markers of pyroptosis,<sup>44,46</sup> are also associated with ΔPK-induced melanoma oncolysis *in vivo*.

#### Discussion

The salient feature of the data presented in this report is the finding that the ICP10PK-deleted virus ΔPK kills melanoma cells in culture and in animal models through

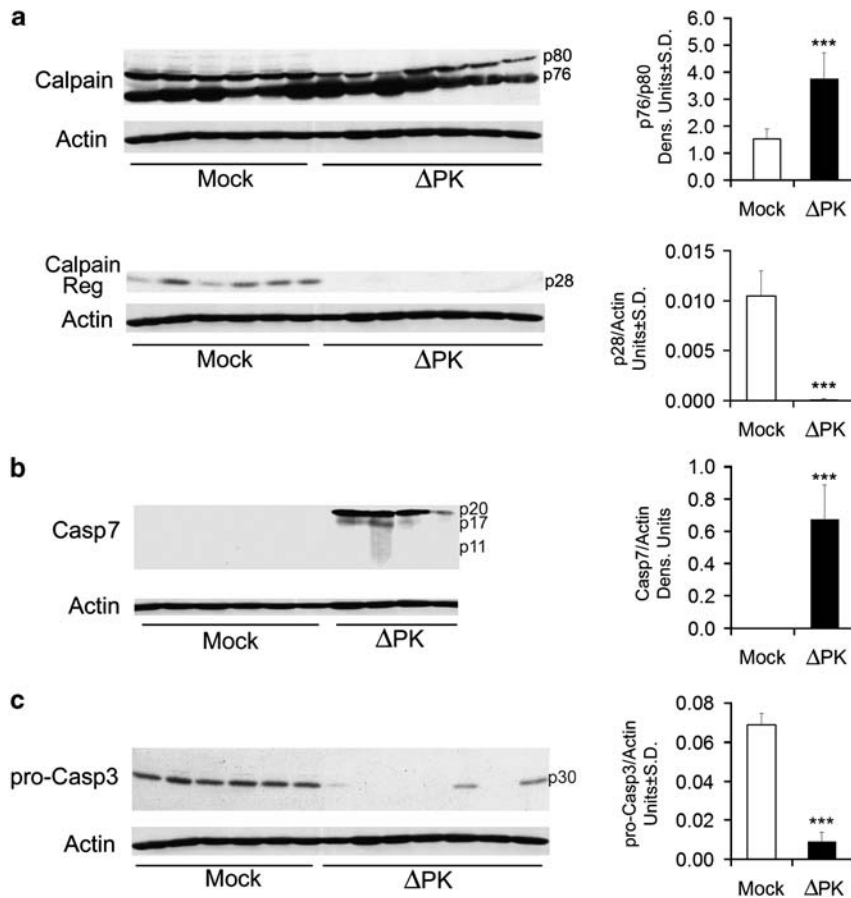


**Figure 6** Calpain and caspases-7 and -3 are activated in  $\Delta$ PK-treated xenografts. A2058 xenograft tissues mock-treated or treated with  $\Delta$ PK as in Figure 5a were collected 7 days after the last  $\Delta$ PK injection and extracts were immunoblotted with antibodies to calpain (a) stripped and sequentially re-blotted with antibodies to activated caspase-7 (b), pro-caspase-3 (c) and actin. Each lane represents a different tumor. Representatives of three replicate experiments are shown for each antibody. Data were quantified by densitometric scanning as described in Materials and methods, and results are expressed as densitometric units (\*\*\*) $P < 0.001$  vs mock).

activation of functionally distinct proteases (nonredundant PCD pathways) and in association with upregulation of Beclin-1, H11/HspB8 and caspase-1-related inflammation. The following comments seem pertinent with respect to these findings.

Oncolytic viruses are engineered and selected to exploit genetic defects in tumor cells that enable selective virus replication. They are designed to reduce the tumor burden by cell lysis resulting from virus replication and the generation of infectious virus progeny that spreads throughout the tumor mass.<sup>3,4</sup> Their therapeutic promise includes the ability to lyse cancer stem cells<sup>2,5</sup> and stimulate antitumor immunity.<sup>3,4</sup> HSV is a particularly promising oncolytic virus because it has a broad host spectrum, is cytolytic, its genome does not integrate into the cellular genome precluding insertion mutagenesis and antiviral drugs are available to safeguard against unfavorable virus replication. However, cumulative data, including early clinical trials, indicate that the therapeutic benefits of virotherapy are modest.<sup>6</sup> As oncolytic viruses are expected to spread through the tumor mass lysing the cells through productive replication, their limited efficacy was attributed to inhibition of replication by antiviral immunity, incomplete dissemination in the tumor mass, and the failure to replicate in quiescent cells, which are the majority of cells in the tumor at any one

time.<sup>48,49</sup> Although ongoing efforts are focused on improving virus replication, it is becoming increasingly evident that the development of oncolytic viruses with distinct molecular death functions is highly desirable.

Our studies follow on recent findings that cancer cell death enhances the penetration and efficacy of oncolytic viruses.<sup>12</sup> They are based on the proposition that oncolytic viruses that induce multiple PCD pathways, which are not the direct outcome of productive virus replication, have increased therapeutic efficacy and are not subject to the limitations currently ascribed to canonical virotherapy. We focused on melanoma, a highly aggressive and drug-resistant cancer of neural crest origin that does not respond to replication-based conventional virotherapy,<sup>14,50</sup> and on  $\Delta$ PK, an HSV-2 mutant that triggers apoptosis in neurons.<sup>22</sup>  $\Delta$ PK differs from the recently described HSV-2 oncolytic construct FusOn-H2, both in its construction and properties.  $\Delta$ PK is deleted in the ICP10 kinase catalytic domain but it retains its transmembrane domain, which is required for membrane localization, protein function and virion stability.<sup>33,51–53</sup> The kinase-deleted ICP10 protein (also known as p95) is present in the virion tegument preserving the structural integrity required for optimal virus uptake and thereby, tumor penetration.<sup>51</sup> p95 expression is directed by the authentic ICP10 promoter

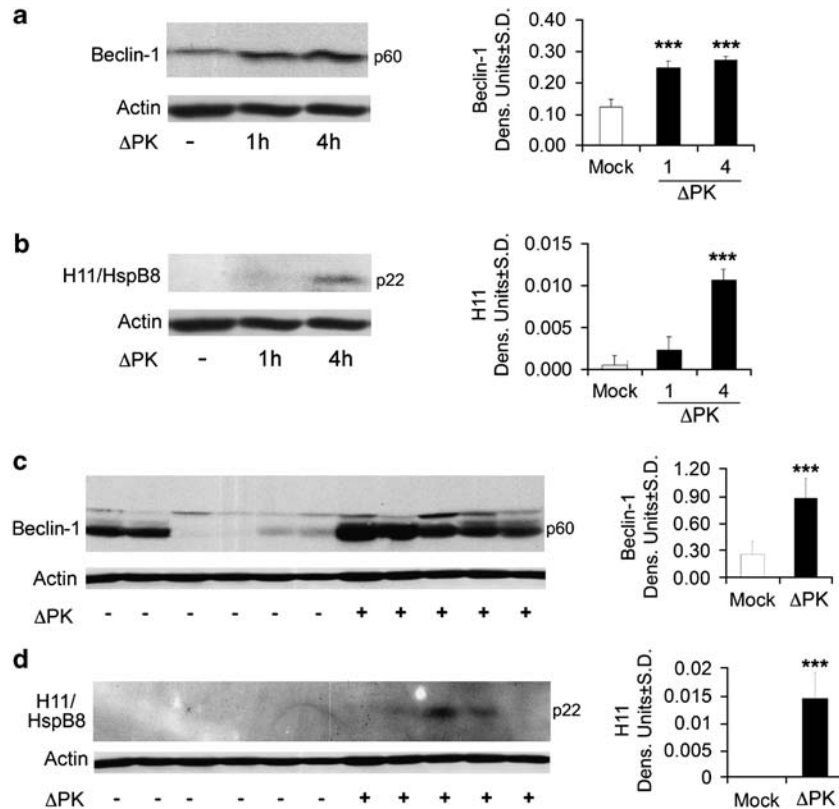


**Figure 7** Beclin-1 and H11/HspB8 are upregulated in  $\Delta$ PK-treated cultures and xenografts. A2058 cultures were infected with  $\Delta$ PK (multiplicity of infection (moi) = 0.5) and cell extracts obtained at various times post-infection were immunoblotted with antibody to Beclin-1 (a), stripped and re-probed with antibodies to H-11/HspB8 (b) and actin. Duplicates of the A2058 xenografts examined for calpain and caspase activation in Figure 7 were immunoblotted with antibody to Beclin-1 (c) stripped and re-probed with antibodies to H11/HspB8 (d) and actin. Each lane represents a different tumor. Representatives of three replicate experiments are shown for each antibody. Data were quantified by densitometric scanning as described in Materials and methods, and results are expressed as densitometric units (\*\*\*)  $P < 0.001$  vs mock).

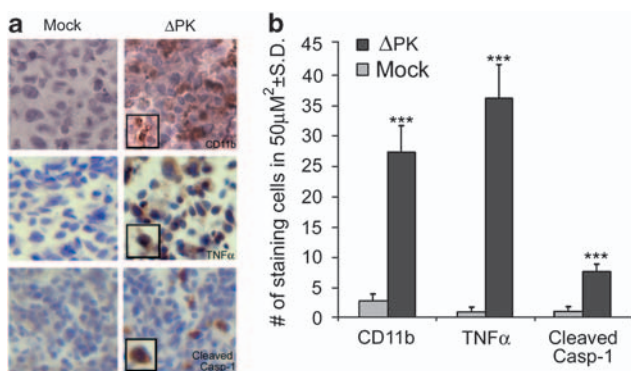


**Figure 8**  $\Delta$ PK-xenografts evidence inflammatory processes. (a) Duplicates of the A2058 xenografts in Figure 6 were stained with antibodies to CD11b (macrophage marker), tumor-necrosis factor alpha (TNF- $\alpha$ ) or activated caspase-1 (caspase-1p20) by immunohistochemistry and counterstained with Mayer's hematoxylin. (b) Staining cells were counted in three randomly selected fields (50  $\mu$ m<sup>2</sup>) and the mean number of positive cells per area was calculated (\*\*\*)  $P < 0.001$  vs mock).

that has IE kinetics and responds to AP-1 transcription factors,<sup>54</sup> which regulate genes involved in tumor cell apoptosis.<sup>55</sup>  $\Delta$ PK does not have any genetic defect other than this deletion,<sup>33,34</sup> and it has the distinct advantages of: (i) inducing a Th1 response<sup>28</sup> that can override the melanoma Th2-based immunosuppressive milieu,<sup>15,29</sup>

and (ii) being tolerated well in humans.<sup>30,31</sup> FusOn-H2 differs from  $\Delta$ PK in that both the ICP10PK catalytic and transmembrane domains were replaced with GFP and the resulting protein was placed under the direction of the promiscuous CMV promoter. Most importantly, the virus was selected for fusogenic activity imparted by an unrelated and uncharacterized genetic alteration that is credited with improved virus replication within tumor cells and oncolytic activity.<sup>7,56</sup> Although DNA fragmentation with 3'-OH ends (TUNEL) was reported in one FusOn-H2-treated tumor,<sup>57</sup> fusogenic activity is considered to be a critical mechanism of oncolysis, as reflected by the virus name.<sup>7,56</sup>

Unlike HSV-2 and HSV-2(R) that replicated equally well in all the examined cell types,  $\Delta$ PK had selective growth potential in cancer/transformed cells. It replicated in melanoma and Vero cells, but not in normal fibroblasts (WI-38) and melanocytes, at least under the conditions used in these studies. This was not due to the absence of infection, because the percentage of cells staining with antibody to ICP10, which is an IE protein that is expressed in the absence of other viral proteins,<sup>37,38</sup> was similar to that seen in the melanoma and Vero cultures and consistent with that expected for the used moi. The maximal levels of virus growth in the melanoma cultures was significantly lower than that of  $\Delta$ PK-induced cell death, with a trypan blue+ or EtHD+/VP5+ ratio of 1.8–4.1 for the different cultures at 24–72 h



p.i., and similar results were obtained for melanoma cultures with distinct patterns of activated survival/proliferation pathways. As VP5 staining is a marker of infectious progeny production, the data suggest that cell death was primarily due to a program other than lysis caused by productive virus growth (replication bystander effect). We conclude that the bystander effect was due to activation of nonredundant death programs because: (i) calpain and caspases-7 and -3 were activated in  $\Delta$ PK<sup>-</sup>, but not mock-infected cultures, and (ii) cell death was reduced by the calpain inhibitor PD150606 or the pancaspase inhibitor z-VAD-fmk (used at previously established effective doses), but it was only abrogated by the combination of both inhibitors. Calpain activation was first seen at 1 h p.i., when it presented as an increased p76/p80 ratio. It increased with time and, by 24 h p.i., was accompanied by the loss of the regulatory p28 subunit. Interestingly, although caspases-7 and -3 generally compensate for each other and are not simultaneously activated, our data indicate that both were activated by  $\Delta$ PK. Activation of caspase-7, was first seen at 4 h p.i. and it increased with time, such that by 24 h p.i., the p20 cleavage fragment was replaced by the lower fragments p17 and p11. Caspase-3 activation was not seen before 24 h p.i. This is consistent with recent reports that these two caspases are differentially activated<sup>58</sup> and they have distinct functions/targets,<sup>40</sup> such that maximal cell death is only seen when both are simultaneously activated.<sup>59</sup>

Apoptosis is the best studied PCD and it involves both caspase-dependent extrinsic and intrinsic pathways.<sup>16</sup> However, canonical apoptosis (measured by TUNEL+ cells) was a relatively small component of the  $\Delta$ PK-induced cell death. Caspase-independent death pathways were also reported, for example, through AIF release from the mitochondria and its translocation to the nucleus,<sup>17,27</sup> as was death caused by both caspase-dependent and -independent pathways<sup>60,61</sup> or by distinct PCD pathways, such as autophagy.<sup>62</sup> Calpains are Ca<sup>2+</sup>-dependent neutral cysteine proteases, the relationship of which to the caspases is still poorly understood. Some reports suggest that calpains act independently of the caspases in different PCD pathways, whereas others conclude that they cooperate. In the latter case, calpain activation was found to follow or initiate the activation of the caspases.<sup>27,63</sup> Calpain cleavage of caspases-9 and -3 was reported to attenuate or facilitate their activity during apoptosis,<sup>42,43</sup> but more recent data suggest that calpains function in caspase-independent PCD.<sup>60,64,65</sup> As activation of calpain and caspase-7 preceded the onset of  $\Delta$ PK replication, although activation of caspase-3 was a relatively late event, we assume that distinct virus functions are involved in the activation of the three proteases, at least some of which are independent of a fully productive replicative cycle. In this context, it is important to point out that expression of the IE protein ICP0 was shown to act as an initial inducer of apoptosis,<sup>66</sup> but the contribution of cellular genes<sup>67</sup> that are likely upregulated by distinct virus functions cannot be excluded. Ongoing studies are designed to examine additional melanoma cultures, determine the relative contribution of caspase-7 vs caspase-3 towards melanoma cell death and identify the virus genes/functions that differentially activate the distinct proteases in  $\Delta$ PK-infected melanoma cultures.

Significantly,  $\Delta$ PK had robust oncolytic activity in melanoma xenografts. The virus was given at a relatively low dose (10<sup>6</sup>–10<sup>7</sup> pfu) but in repeated weekly intratumoral injections, a protocol selected to: (i) favor safety while improving tumor penetration through repeated exposure<sup>68</sup> and (ii) reduce the risk of developing virus-resistant melanoma cells resulting from poor killing, as previously described.<sup>14</sup> Although these studies were limited to three melanoma cultures (A2058, A375 and LM), tumor growth was inhibited in all cases with virtually absolute survival (80–100%). In the case of the LM xenografts, complete remission was seen for seven of eight tumors (87.5%) followed for 5 months after the last  $\Delta$ PK injection and the lone recurrent tumor did not reach end-point criteria (1.5 cm in diameter) by this time.

Analysis of the  $\Delta$ PK-treated xenografts at 7 days after the last injection indicated that a small number of well distributed cells stained with VP5 antibody and the tissues were positive for low titers of infectious virus, indicative of sustained virus replication and relatively good levels of tumor penetration. As was the case for the melanoma cultures, the  $\Delta$ PK-treated xenografts were positive for activated calpain and caspases-7 and -3. Interestingly, they also evidenced upregulation of Beclin-1 and H11/HspB8. We conclude that this is not an artifact of the tumor microenvironment, because both proteins were also upregulated in  $\Delta$ PK-infected melanoma cultures. In addition, the  $\Delta$ PK-treated xenografts were also positive for activated caspase-1 and evidenced increased levels of the pro-inflammatory cytokine TNF- $\alpha$  and infiltrating CD11b+ cells (macrophages). In this context, it is important to point out that the caspase-1 antibody used in these studies is specific for the human protein, suggesting that the activated caspase-1 detected in the  $\Delta$ PK-treated xenografts is of melanoma, rather than macrophage origin. The exact contribution of these death-related proteins to melanoma oncolysis is still unclear, but presently available data underscore their potential cross talk with caspase and/or calpain-induced PCD. Autophagy is a process of self-digestion that was reported to cause or protect against cell death<sup>69,70</sup> and calpain can cleave autophagy proteins, thereby providing a switch between autophagy and apoptosis.<sup>18</sup> The critical autophagy protein Beclin-1 was associated with cell death involving cross talk with Bcl-2 family members<sup>70</sup> and it acts as a haploinsufficient tumor suppressor protein that is downregulated in human tumors.<sup>20,21</sup> Pyroptosis is a caspase-1-dependent inflammatory form of cell death that involves formation of the inflammasome complex and was originally observed in macrophages.<sup>44,45</sup> TNF- $\alpha$ , a pro-apoptotic inflammatory cytokine is a death signal and it slows the growth of some tumors.<sup>47</sup> TNF- $\alpha$  can also activate caspase-1<sup>19</sup> and caspase-7 is a caspase-1 substrate.<sup>58</sup> The finding that these death-associated factors coexist with protease activation suggests that they are likely to be independently upregulated/activated by  $\Delta$ PK and contribute to oncolysis *in vivo*, possibly through a positive feedback amplification loop. However, because in cultured cells, oncolysis is abolished through caspase and calpain inhibition, we cannot exclude the possibility that Beclin-1, H11/HspB8 and the inflammatory processes function downstream of calpain and/or caspase. Infectious virus and VP5 staining were not seen in the liver

tissues collected at the end of the experimental procedure (data not shown), indicating that there was no systemic toxicity. In fact,  $\Delta$ PK was also well tolerated in early clinical trials.<sup>30,31</sup>

Collectively, the data indicate that  $\Delta$ PK is a promising melanoma virotherapy strategy in which the relatively limited virus replication is associated with a robust tumor cell killing bystander effect apparently mediated by alternative PCD programs. Ongoing studies are designed to elucidate the role of the various death programs in melanoma cell death in culture and *in vivo*, to verify whether they differ for distinct melanoma cultures, to examine whether virus-resistant cells, including nestin-1+ cancer stem cells emerge during the course of virotherapy and to determine the role of tumor associated antigens (TAA) load and tumor immunity in the oncolytic activity of  $\Delta$ PK.

## Materials and methods

### Cells and viruses

Melanoma cell lines A2058, A375, MeWo and SKMEL-2 were obtained from the American Type Culture Collection (ATCC, Manassas, VA, USA) and grown in Dulbecco's modified Eagle's medium with 10% FBS (Gemini Bioproducts, Calabasos, CA, USA). For A375, A2058 and MeWo, the medium was supplemented with 4.5 g l<sup>-1</sup> glucose, 1500 mg ml<sup>-1</sup> sodium bicarbonate and 4 mM glutamine. Melanoma cultures LM, SM, LN, OV and BUL were established from histologically confirmed metastatic melanomas and passaged only four to six times before study. SM, LN, OV and BUL were obtained from Dr G Elias (Franklin Square Hospital, Baltimore, MD, USA) and cultured in Iscove's Modified Dulbecco's Medium. LM were obtained from Dr Joseph Sinkovics (University of South Florida, Tampa, FL, USA) and cultured in RPMI 1640 medium with 10% FBS. Adult primary melanocytes (Cascade Biologics/Invitrogen, Portland, OR, USA) were grown in Medium 254 supplemented with 0.5% fetal bovine serum, 3 ng ml<sup>-1</sup> basic fibroblast growth factor, 0.2% bovine pituitary extract, 3  $\mu$ g ml<sup>-1</sup> heparin, 0.18  $\mu$ g ml<sup>-1</sup> hydrocortisone, 5  $\mu$ g ml<sup>-1</sup> insulin, 5  $\mu$ g ml<sup>-1</sup> transferrin and 10 nM endothelin-1 (human melanocyte supplement-2 from Cascade Biologics). WI-38 cells (normal human embryonic lung fibroblasts, ATCC) are an expansion from passage 9 and have a limited lifespan of 50 population doublings. Vero cells (African green monkey kidney, ATCC) were used at a relatively late passage (>150) at which they evidence transformation-related properties and tumor formation.<sup>36</sup> WI-38 and Vero cells were cultured in minimal essential medium with Earle's salts, 10% FBS, 1 mM sodium pyruvate and 0.1 mM nonessential amino acids.

The generation and properties of the HSV-2 mutant  $\Delta$ PK and the revertant virus HSV-2(R) were previously described.<sup>33</sup>  $\Delta$ PK is deleted in the sequences that encode the kinase function of ICP10 (also known as HSV-2 R1). The ICP10 kinase activity functions independently of the R1 activity and is required for virus growth.  $\Delta$ PK expresses the kinase-negative (ICP10PK deleted) protein p95 under the direction of the authentic IE ICP10 promoter.<sup>33</sup>  $\Delta$ PK was grown in Vero cells. Cell lysates were cleared of cell debris by centrifugation at 3000 g for 10 min. Virus was used as it is or further partially

purified by centrifugation of the cell lysates at 113 000 g for 1 h followed by resuspension in minimal essential medium with Earle's salts, 1 mM sodium pyruvate and 0.1 mM nonessential amino acids, as previously described.<sup>39</sup>

### Antibodies, pharmacological inhibitors and chemical reagents

The generation and specificity of the rabbit polyclonal antibodies to ICP10, which recognizes an epitope that is retained by both ICP10 and the PK deleted ICP10 protein p95<sup>22-27,33,34</sup> and H11/HspB8<sup>32</sup> were previously described. The following antibodies were purchased and used according to manufacturer's instructions. Antibodies to caspase-3 (recognizes both the zymogen and its cleavage products), activated caspase-3 (caspase-3 p20), calpain (p80, p78, p28), Beclin-1, ERK1/2, activated human caspase-1, and actin were purchased from Santa Cruz Biotechnology (Santa Cruz, CA, USA). Antibodies to activated caspase-7, phosphorylated (activated) Akt (pAkt) and total Akt were purchased from Cell Signaling Technology (Danvers, MA, USA), antibody to phosphorylated (activated) ERK 1/2 (pERK1/2) from Promega, antibody to CD11b (Mac-1<sub>m</sub> chain-biotin conjugated) from Leinco (St Louis, MO, USA), antibody to the HSV major capsid protein VP5 from Virusys Corporation (Sykesville, MD, USA) and antibody to TNF- $\alpha$  from R&D Systems (Minneapolis, MN, USA). Alexafluor 594-conjugated anti-mouse and Alexafluor 488-conjugated anti-rabbit secondary antibodies were purchased from Invitrogen (Carlsbad, CA, USA). Horseradish peroxidase-conjugated anti-rabbit and anti-mouse antibodies were purchased from Cell Signaling Technologies. The *In situ* Cell Death Detection Kit (TUNEL) with fluorescein isothiocyanate-labeled dUTP was purchased from Roche (Indianapolis, IN, USA), the calpain inhibitor PD150606 from Calbiochem (La Jolla, CA, USA) and the pancaspase inhibitor z-VAD-fmk from Sigma-Aldrich and Promega.

### Virus growth

To measure virus replication in culture, the cells were infected at a moi of 0.5 pfu per cell. Adsorption was for 1 h at 4 °C (synchronized infection). At this time, virus was removed and the cells were overlaid with minimal essential medium with 0 or 10% FBS (0 h p.i.). They were collected at various times p.i. and virus was released by seven freeze-thaw cycles and sonication (60 s at 25% output power using a Sonicator/Ultrasonic processor (Misonix, Inc., Farmingdale, NY, USA)). Virus titers were determined by plaque assay on Vero cells and the results are expressed as mean pfu per cell (burst size), as described.<sup>32</sup> To determine the titers of infectious virus in  $\Delta$ PK-treated xenografts, tissues (15 mg samples) collected at 7 days after the last injection were suspended in 50  $\mu$ l of virus adsorption medium (PBS supplemented with 0.2% glucose and 0.2% bovine serum albumin (BSA)) and homogenized on ice using a sterile pre-chilled micro-pestle. The homogenates were cleared of cell debris by centrifugation (3000 g, 10 min, 4 °C) and virus titers were determined by plaque assay.

### Immunofluorescence and immunohistochemistry

For immunofluorescence, cells grown on glass coverslips were fixed with 4% paraformaldehyde overnight at 4 °C. They were then blocked with 5% normal goat serum and

5% BSA (30 min at room temperature) and incubated with primary antibody overnight at 4 °C. They were washed in PBS with 0.1% Tween 20, exposed to fluorochrome-labeled secondary antibodies (37 °C, 1 h) and mounted in Vectashield with 4,6-diamidino-2-phenylindole (DAPI) (Vector Laboratories, Burlingame, CA, USA). Slides were visualized with an Olympus BX50 fluorescence microscope (Center Valley, PA, USA) using fluorescein isothiocyanate (330–380 nm), UV (for DAPI) (465–495 nm) and Texas red (540–580 nm) cubes. The stained cells were counted in five randomly selected 3 mm<sup>2</sup> fields ( $\geq 250$  cells each) and the percentage of positive cells was calculated relative to total number of cells imaged by DAPI, as previously described.<sup>23–27</sup> For immunohistochemistry, tumor sections were postfixed (30 min) in 4% paraformaldehyde in PBS (w/v), treated (10 min) with 0.3% H<sub>2</sub>O<sub>2</sub> to remove endogenous peroxidases, permeabilized and blocked in blocking solution (10% goat serum, 1% BSA and 0.3% Triton-X 100 in PBS) for 1 h. Sections (20 μm) were exposed overnight (4 °C) to the primary antibody diluted in blocking solution followed by horseradish peroxidase-conjugated secondary antibody diluted in 5% goat serum and 5% BSA (1 h). The reaction was developed with ImmPACT DAB substrate (Vector Laboratories) and the sections were counterstained with Mayer's hematoxylin (Sigma-Aldrich). They were dehydrated and mounted in Permount (Sigma-Aldrich). Visualization was with an Olympus BX50 microscope under brightfield conditions. The stained cells were counted in representative 50 μm<sup>2</sup> fields in each of four tumors/treatment and the percentage of positive cells was calculated relative to the total cells per field, as described.<sup>23–27,34,46</sup>

#### Cell death and TUNEL

Cell death was determined by trypan blue exclusion and staining with Ethidium homodimer-1 (EtHD-1), a cell impermeable red fluorescent nuclear stain that increases intensity after binding to the DNA of dead cells. For trypan blue staining, cells were collected by centrifugation and the pellet was resuspended in 50 μl PBS to which 50 μl trypan blue was added. Dead cells were counted by four independent hemocytometer counts. EtHD-1 staining was carried out as per manufacturer's instructions and visualized by microscopy at ×4 magnification using a Nikon E4100 fluorescent microscope (Melville, NY, USA) using phase contrast and a Texas red (540–580 nm) cube. The stained cells were counted in five randomly selected 3 mm<sup>2</sup> fields ( $\geq 250$  cells each), and the percentage of positive cells was calculated relative to total number of cells imaged by phase contrast microscopy.<sup>24</sup> Detection of apoptotic DNA fragmentation with 3'-OH ends by TUNEL assay used the *In situ* Cell Death Detection kit (Roche) as per the manufacturer's instructions.

#### Immunoblotting

Cultured cells were lysed with radioimmunoprecipitation buffer (RIPA; 20 mM Tris-HCl (pH 7.4), 0.15 mM NaCl, 1% Nonidet P-40, 0.1% SDS, 0.5% sodium deoxycholate) supplemented with protease and phosphatase inhibitor cocktails (Sigma-Aldrich) and sonicated twice for 30 s at 25% output power with a Sonicator ultrasonic processor (Misonix, Inc.). Xenograft tissues were weighed, resuspended in RIPA buffer (0.5 ml g<sup>-1</sup>),

homogenized using a pre-chilled motorized pestle (Kontes, Vineland, NJ, USA) and cleared of cell debris by centrifugation (10 000 g; 4 °C for 30 min). Protein concentrations were determined by the bicinchoninic assay (Pierce, Rockford, IL, USA) and 100 μg protein samples were resolved by SDS-polyacrylamide gel electrophoresis and transferred to polyvinylidene fluoride membranes. Immunoblotting was as previously described.<sup>22–27,33,34,51–54</sup> Briefly, membranes were blocked (1 h, room temperature) in 5% nonfat milk in TN-T buffer (0.01 M Tris-HCl pH 7.4, 0.15 M NaCl, 0.05% Tween-20), exposed (1 h) to primary antibodies, washed in TN-T buffer and incubated (1 h) in horseradish peroxidase-conjugated secondary antibodies. Detection was with ECL reagents (Amersham, Pittsburg, PA, USA) and high-performance chemiluminescence film (Hyperfilm ECL, Amersham). Quantitation was by densitometric scanning with the Bio-Rad GS-700 imaging densitometer (Bio-Rad, Hercules, CA, USA). The results of three independent experiments are expressed as the mean actin-adjusted densitometric units ± s.d.

#### In vivo studies.

The Animal Care and Use Committee of the University of Maryland School of Medicine approved all the described studies. Male nude mice (6 to 8-week-old) (Balb/c nu/nu) were obtained from Charles River Laboratories (Wilmington, MA, USA). To establish subcutaneous melanoma xenograft models, nude mice were given A2058, A375 or LM melanoma cells (10<sup>7</sup> in 100 μl) by subcutaneous injection into both the left and right hind flanks. When the tumors became palpable (~200 mm<sup>3</sup> in volume; day 14 for A2058 and day 7 for A375 and LM xenografts), animals were randomly assigned to treatment groups. Treatments consisted of intratumoral injections of partially purified ΔPK (10<sup>6</sup> or 10<sup>7</sup> pfu) in a total volume of 100 μl of cell culture medium or 100 μl of virus-free culture medium (control). The treatment protocol consisted of four injections given at weekly intervals (one injection per week). Every other day, minimum and maximum perpendicular tumor axes were measured with microcalipers and tumor volume was calculated using the formula: volume = ((length × width<sup>2</sup>)/2). Animals were maintained in pathogen-free conditions and were euthanized when their tumors reached 1.5 cm in any one direction. Tissues were collected after euthanasia, and processed for virus titration, staining and immunoblotting.

#### Statistical analysis

Analysis of variance (ANOVA) was carried out with SigmaStat version 3.1 for Windows (Systat Software, Point Richmond, CA, USA). Tumor volumes were compared over time between untreated and treated groups by pairwise two-way ANOVA followed by the Tukey's honestly significant difference test. Kaplan-Meier survival analysis was carried out with 1.5 cm of tumor growth in any one dimension as the terminal event and curve comparison was by Log-Rank (Mantel-Cox) analysis.

#### Conflict of interest

The authors declare no conflict of interest.

## Acknowledgements

We thank Dr Cynthia Smith for her thoughtful help and advice. These studies were supported by the Public health Service Grant AR053512 from NIAMS, NIH. AC was supported by Grant ES07263 from NIEHS, NIH.

## References

- Jemal A, Siegel R, Ward E, Murray T, Xu J, Thun MJ. Cancer statistics, 2007. *CA Cancer J Clin* 2007; **57**: 43–66.
- Schatton T, Frank MH. Cancer stem cells and human malignant melanoma. *Pigment Cell Melanoma Res* 2008; **21**: 39–55.
- Shen Y, Nemunaitis J. Herpes simplex virus 1 (HSV-1) for cancer treatment. *Cancer Gene Ther* 2006; **13**: 975–992.
- Mathis JM, Stoff-Khalili MA, Curiel DT. Oncolytic adenoviruses—selective retargeting to tumor cells. *Oncogene* 2005; **24**: 7775–7791.
- Ribacka C, Pesonen S, Hemminki A. Cancer, stem cells, and oncolytic viruses. *Ann Med* 2008; **40**: 496–505.
- Aghi M, Martuza RL. Oncolytic viral therapies—the clinical experience. *Oncogene* 2005; **24**: 7802–7816.
- Fu X, Tao L, Cai R, Prigge J, Zhang X. A mutant type 2 herpes simplex virus deleted for the protein kinase domain of the ICP10 gene is a potent oncolytic virus. *Mol Ther* 2006; **13**: 882–890.
- Kurozumi K, Hardcastle J, Thakur R, Yang M, Christoforidis G, Fulci G et al. Effect of tumor microenvironment modulation on the efficacy of oncolytic virus therapy. *J Natl Cancer Inst* 2007; **99**: 1768–1781.
- Fulci G, Breyman L, Gianni D, Kurozumi K, Rhee SS, Yu J et al. Cyclophosphamide enhances glioma virotherapy by inhibiting innate immune responses. *Proc Natl Acad Sci USA* 2006; **103**: 12873–12878.
- Hu JC, Coffin RS, Davis CJ, Graham NJ, Groves N, Guest PJ et al. A phase I study of OncoVEXGM-CSF, a second-generation oncolytic herpes simplex virus expressing granulocyte macrophage colony-stimulating factor. *Clin Cancer Res* 2006; **12**: 6737–6747.
- Kumar S, Gao L, Yeagy B, Reid T. Virus combinations and chemotherapy for the treatment of human cancers. *Curr Opin Mol Ther* 2008; **10**: 371–379.
- Nagano S, Perentes JY, Jain RK, Boucher Y. Cancer cell death enhances the penetration and efficacy of oncolytic herpes simplex virus in tumors. *Cancer Res* 2008; **68**: 3795–3802.
- Del Bello B, Moretti D, Gamberucci A, Maellaro E. Cross-talk between calpain and caspase-3/-7 in cisplatin-induced apoptosis of melanoma cells: a major role of calpain inhibition in cell death protection and p53 status. *Oncogene* 2007; **26**: 2717–2726.
- Vaha-Koskela MJ, Kallio JP, Jansson LC, Heikkilä JE, Zakhartchenko VA, Kallajoki MA et al. Oncolytic capacity of attenuated replicative semliki forest virus in human melanoma xenografts in severe combined immunodeficient mice. *Cancer Res* 2006; **66**: 7185–7194.
- Polak ME, Borthwick NJ, Gabriel FG, Johnson P, Higgins B, Hurren J et al. Mechanisms of local immunosuppression in cutaneous melanoma. *Br J Cancer* 2007; **96**: 1879–1887.
- Aurelian L. HSV-induced apoptosis in herpes encephalitis. *Curr Top Microbiol Immunol* 2005; **289**: 79–111.
- Chu CT, Zhu JH, Cao G, Signore A, Wang S, Chen J. Apoptosis inducing factor mediates caspase-independent 1-methyl-4-phenylpyridinium toxicity in dopaminergic cells. *J Neurochem* 2005; **94**: 1685–1695.
- Luo S, Rubinsztein DC. Atg5 and Bcl-2 provide novel insights into the interplay between apoptosis and autophagy. *Cell Death Differ* 2007; **14**: 1247–1250.
- Jain N, Sudhakar C, Swarup G. Tumor necrosis factor-α-induced caspase-1 gene expression. Role of p73. *FEBS J* 2007; **274**: 4396–4407.
- Qu X, Yu J, Bhagat G, Furuya N, Hibshoosh H, Troxel A et al. Promotion of tumorigenesis by heterozygous disruption of the Beclin 1 autophagy gene. *J Clin Invest* 2003; **112**: 1809–1820.
- Miracco C, Cosci E, Oliveri G, Luzi P, Pacenti L, Monciatti I et al. Protein and mRNA expression of autophagy gene Beclin 1 in human brain tumours. *Int J Oncol* 2007; **30**: 429–436.
- Perkins D, Pereira EF, Aurelian L. The herpes simplex virus type 2 R1 protein kinase (ICP10 PK) functions as a dominant regulator of apoptosis in hippocampal neurons involving activation of the ERK survival pathway and upregulation of the antiapoptotic protein Bag-1. *J Virol* 2003; **77**: 1292–1305.
- Laing JM, Gober MD, Golembewski EK, Thompson SM, Gyure KA, Yarowsky PJ et al. Intranasal administration of the growth-compromised HSV-2 vector DeltaRR prevents kainate-induced seizures and neuronal loss in rats and mice. [published erratum appears in *Mol Ther* 2007; **15**: 1734]. *Mol Ther* 2006; **13**: 870–881.
- Gober MD, Laing JM, Thompson SM, Aurelian L. The growth-compromised HSV-2 mutant DeltaRR prevents kainic acid-induced apoptosis and loss of function in organotypic hippocampal cultures. *Brain Res* 2006; **1119**: 26–39.
- Golembewski EK, Wales SQ, Aurelian L, Yarowsky PJ. The HSV-2 protein ICP10PK prevents neuronal apoptosis and loss of function in an *in vivo* model of neurodegeneration associated with glutamate excitotoxicity. *Exp Neurol* 2007; **203**: 381–393.
- Wales SQ, Li B, Laing JM, Aurelian L. The herpes simplex virus type 2 gene ICP10PK protects from apoptosis caused by nerve growth factor deprivation through inhibition of caspase-3 activation and XIAP up-regulation. *J Neurochem* 2007; **103**: 365–379.
- Wales SQ, Laing JM, Chen L, Aurelian L. ICP10PK inhibits calpain-dependent release of apoptosis-inducing factor and programmed cell death in response to the toxin MPP+. *Gene Therapy* 2008; **15**: 1397–1409.
- Gyotoku T, Ono F, Aurelian L. Development of HSV-specific CD4+ Th1 responses and CD8+ cytotoxic T lymphocytes with antiviral activity by vaccination with the HSV-2 mutant ICP10DeltaPK. *Vaccine* 2002; **20**: 2796–2807.
- Minkis K, Kavanagh DG, Alter G, Bogunovic D, O'Neill D, Adams S et al. Type 2 bias of T cells expanded from the blood of melanoma patients switched to type 1 by IL-12p70 mRNA-transfected dendritic cells. *Cancer Res* 2008; **68**: 9441–9450.
- Casanova G, Cancela R, Alonzo L, Benuto R, Magana Mdel C, Hurley DR et al. A double-blind study of the efficacy and safety of the ICP10deltaPK vaccine against recurrent genital HSV-2 infections. *Cutis* 2002; **70**: 235–239.
- Aurelian L. Herpes simplex virus type 2 vaccines: new ground for optimism? *Clin Diagn Lab Immunol* 2004; **11**: 437–445.
- Li B, Smith CC, Laing JM, Gober MD, Liu L, Aurelian L. Overload of the heat-shock protein H11/HspB8 triggers melanoma cell apoptosis through activation of transforming growth factor-beta-activated kinase 1. *Oncogene* 2007; **26**: 3521–3531.
- Smith CC, Peng T, Kulka M, Aurelian L. The PK domain of the large subunit of herpes simplex virus type 2 ribonucleotide reductase (ICP10) is required for immediate-early gene expression and virus growth. *J Virol* 1998; **72**: 9131–9141.
- Smith CC, Nelson J, Aurelian L, Gober M, Goswami BB. Ras-GAP binding and phosphorylation by herpes simplex virus type 2 RR1 PK (ICP10) and activation of the Ras/MEK/MAPK mitogenic pathway are required for timely onset of virus growth. *J Virol* 2000; **74**: 10417–10429.
- Omholt K, Platz A, Kanter L, Ringborg U, Hansson J. NRAS and BRAF mutations arise early during melanoma pathogenesis and are preserved throughout tumor progression. *Clin Cancer Res* 2003; **9**: 6483–6488.
- Manohar M, Orrison B, Peden K, Lewis Jr AM. Assessing the tumorigenic phenotype of VERO cells in adult and newborn nude mice. *Biologicals* 2008; **36**: 65–72.
- Wymer JP, Chung TD, Chang YN, Hayward GS, Aurelian L. Identification of immediate-early-type cis-response elements in

- the promoter for the ribonucleotide reductase large subunit from herpes simplex virus type 2. *J Virol* 1989; **63**: 2773–2784.
- 38 Knipe DM, Fields BN, Howley PM, Griffin D, Lamb R, Martin MA. *Fields' Virology*. Wolters Kluwer Health/Lippincott Williams & Wilkins: Philadelphia, PA c2007 2007, pp 86.
- 39 Sheridan JF, Beck M, Smith CC, Aurelian L. Reactivation of herpes simplex virus is associated with production of a low molecular weight factor that inhibits lymphokine activity *in vitro*. *J Immunol* 1987; **138**: 1234–1239.
- 40 Walsh JG, Cullen SP, Sheridan C, Luthi AU, Gerner C, Martin SJ. Executioner caspase-3 and caspase-7 are functionally distinct proteases. *Proc Natl Acad Sci USA* 2008; **105**: 12815–12819.
- 41 Goll DE, Thompson VF, Li H, Wei W, Cong J. The calpain system. *Physiol Rev* 2003; **83**: 731–801.
- 42 Bizat N, Hermel JM, Humbert S, Jacquard C, Creminon C, Escartin C et al. *In vivo* calpain/caspase cross-talk during 3-nitropropionic acid-induced striatal degeneration: implication of a calpain-mediated cleavage of active caspase-3. *J Biol Chem* 2003; **278**: 43245–43253.
- 43 Neumar RW, Xu YA, Gada H, Guttmann RP, Siman R. Cross-talk between calpain and caspase proteolytic systems during neuronal apoptosis. *J Biol Chem* 2003; **278**: 14162–14167.
- 44 Fernandes-Alnemri T, Wu J, Yu JW, Datta P, Miller B, Jankowski W et al. The pyroptosome: a supramolecular assembly of ASC dimers mediating inflammatory cell death via caspase-1 activation. *Cell Death Differ* 2007; **14**: 1590–1604.
- 45 Yu HB, Finlay BB. The caspase-1 inflammasome: a pilot of innate immune responses. *Cell Host Microbe* 2008; **4**: 198–208.
- 46 Laing JM, Aurelian L. DeltaRR vaccination protects from KA-induced seizures and neuronal loss through ICP10PK-mediated modulation of the neuronal-microglial axis. *Genet Vaccines Ther* 2008; **6**: 1.
- 47 Villeneuve J, Tremblay P, Vallieres L. Tumor necrosis factor reduces brain tumor growth by enhancing macrophage recruitment and microcyst formation. *Cancer Res* 2005; **65**: 3928–3936.
- 48 Aghi M, Visted T, Depinho RA, Chiocca EA. Oncolytic herpes virus with defective ICP6 specifically replicates in quiescent cells with homozygous genetic mutations in p16. *Oncogene* 2008; **27**: 4249–4254.
- 49 Yun CO. Overcoming the extracellular matrix barrier to improve intratumoral spread and therapeutic potential of oncolytic virotherapy. *Curr Opin Mol Ther* 2008; **10**: 356–361.
- 50 MacKie RM, Stewart B, Brown SM. Intralesional injection of herpes simplex virus 1716 in metastatic melanoma. *Lancet* 2001; **357**: 525–526.
- 51 Smith CC, Luo JH, Hunter JC, Ordonez JV, Aurelian L. The transmembrane domain of the large subunit of HSV-2 ribonucleotide reductase (ICP10) is required for protein kinase activity and transformation-related signaling pathways that result in ras activation. *Virology* 1994; **200**: 598–612.
- 52 Luo JH, Aurelian L. The transmembrane helical segment but not the invariant lysine is required for the kinase activity of the large subunit of herpes simplex virus type 2 ribonucleotide reductase (ICP10). *J Biol Chem* 1992; **267**: 9645–9653.
- 53 Smith CC, Aurelian L. The large subunit of herpes simplex virus type 2 ribonucleotide reductase (ICP10) is associated with the virion tegument and has PK activity. *Virology* 1997; **234**: 235–242.
- 54 Gober MD, Wales SQ, Hunter JC, Sharma BK, Aurelian L. Stress up-regulates neuronal expression of the herpes simplex virus type 2 large subunit of ribonucleotide reductase (R1; ICP10) by activating activator protein 1. *J Neurovirol* 2005; **11**: 329–336.
- 55 Royuela M, Rodriguez-Berriguete G, Fraile B, Paniagua R. TNF-alpha/IL-1/NF-kappaB transduction pathway in human cancer prostate. *Histol Histopathol* 2008; **23**: 1279–1290.
- 56 Fu X, Tao L, Zhang X. An oncolytic virus derived from type 2 herpes simplex virus has potent therapeutic effect against metastatic ovarian cancer. *Cancer Gene Ther* 2007; **14**: 480–487.
- 57 Fu X, Tao L, Zhang X. An HSV-2-based oncolytic virus deleted in the PK domain of the ICP10 gene is a potent inducer of apoptotic death in tumor cells. *Gene Therapy* 2007; **14**: 1218–1225.
- 58 Lamkanfi M, Kanneganti TD, Van Damme P, Vanden Berghe T, Vanoverberghe I, Vandekerckhove J et al. Targeted peptide-centric proteomics reveals caspase-7 as a substrate of the caspase-1 inflammasomes. *Mol Cell Proteomics* 2008; **7**: 2350–2363.
- 59 Sung YH, Lee JS, Park SH, Koo J, Lee GM. Influence of co-down-regulation of caspase-3 and caspase-7 by siRNAs on sodium butyrate-induced apoptotic cell death of Chinese hamster ovary cells producing thrombopoietin. *Metab Eng* 2007; **9**: 452–464.
- 60 Choi WS, Lee EH, Chung CW, Jung YK, Jin BK, Kim SU et al. Cleavage of Bax is mediated by caspase-dependent or independent calpain activation in dopaminergic neuronal cells: protective role of Bcl-2. *J Neurochem* 2001; **77**: 1531–1541.
- 61 Han BS, Hong HS, Choi WS, Markelonis GJ, Oh TH, Oh YJ. Caspase-dependent and -independent cell death pathways in primary cultures of mesencephalic dopaminergic neurons after neurotoxin treatment. *J Neurosci* 2003; **23**: 5069–5078.
- 62 Shacka JJ, Roth KA, Zhang J. The autophagy-lysosomal degradation pathway: role in neurodegenerative disease and therapy. *Front Biosci* 2008; **13**: 718–736.
- 63 Gao G, Dou QP. N-terminal cleavage of bax by calpain generates a potent proapoptotic 18-kDa fragment that promotes bcl-2-independent cytochrome C release and apoptotic cell death. *J Cell Biochem* 2000; **80**: 53–72.
- 64 Takano J, Tomioka M, Tsubuki S, Higuchi M, Iwata N, Itohara S et al. Calpain mediates excitotoxic DNA fragmentation via mitochondrial pathways in adult brains: evidence from calpastatin mutant mice. *J Biol Chem* 2005; **280**: 16175–16184.
- 65 Cao G, Xing J, Xiao X, Liou AK, Gao Y, Yin XM et al. Critical role of calpain I in mitochondrial release of apoptosis-inducing factor in ischemic neuronal injury. *J Neurosci* 2007; **27**: 9278–9293.
- 66 Sanfilippo CM, Blaho JA. ICP0 gene expression is a herpes simplex virus type 1 apoptotic trigger. *J Virol* 2006; **80**: 6810–6821.
- 67 Mahller YY, Sakthivel B, Baird WH, Aronow BJ, Hsu YH, Cripe TP et al. Molecular analysis of human cancer cells infected by an oncolytic HSV-1 reveals multiple upregulated cellular genes and a role for SOCS1 in virus replication. *Cancer Gene Ther* 2008; **15**: 733–741.
- 68 Huszthy PC, Goplen D, Thorsen F, Immervoll H, Wang J, Gutermann A et al. Oncolytic herpes simplex virus type-1 therapy in a highly infiltrative animal model of human glioblastoma. *Clin Cancer Res* 2008; **14**: 1571–1580.
- 69 White E. Autophagic cell death unraveled: pharmacological inhibition of apoptosis and autophagy enables necrosis. *Autophagy* 2008; **4**: 399–401.
- 70 Levine B, Sinha S, Kroemer G. Bcl-2 family members: dual regulators of apoptosis and autophagy. *Autophagy* 2008; **4**: 600–606.

Supplementary Information accompanies the paper on Gene Therapy website (<http://www.nature.com/gt>)